ELSEVIER

Journal of Power Sources 112 (2002) 614–620

JOURNAL OF POWER SOURCES

www.elsevier.com/locate/jpowsour

Capacity fade of Sony 18650 cells cycled at elevated temperatures Part II. Capacity fade analysis

P. Ramadass, Bala Haran, Ralph White, Branko N. Popov*

Department of Chemical Engineering, Col. Engineering and Info. Techn., University of South Carolina, Columbia, SC 29208, USA

Received 2 August 2002; accepted 30 August 2002

Abstract

A complete capacity fade analysis was carried out for Sony 18650 cells cycled at elevated temperatures. The major causes of capacity loss were identified and a complete capacity fade balance was carried out to account for the total capacity loss of Li-ion battery as a function of cycle number and temperature. The three most significant parameters that cause capacity loss were loss of secondary active material ($LiCoO_2$/carbon) and primary active material (Li^+) and the rate capability losses. Intrinsic capacity measurements for both positive and negative electrode has been used to estimate the capacity loss due to secondary active material and a charge balance gives the capacity lost due to primary active material (Li^+). Capacity fade has been quantified with secondary active material loss dominating the other losses.

Keywords: Capacity fade; Sony 18650 cells; Cycle number

1. Introduction

Capacity fade of commercial Li-ion battery has been studied in details at ambient conditions [1–5]. The results reported indicated that Li-ion cell performs well at temperatures up to 40 °C. Since the battery loses its capacity at high rate when cycled at elevated temperatures, the capacity fade studies at temperatures higher than 40 °C became crucial for proper use of Li-ion cells in modern electronics that needs the cells to be discharged under temperature that ranges up to 60 °C.

The objective of this paper was to study the change in capacity of commercial Sony 18650 cells when cycled at higher temperatures and to develop a methodology to quantify the capacity loss with cycling. Part I of this series dealt with the cycling performance and capacity fade of Sony 18650 cells at elevated temperatures where an extensive analysis of discharge behavior and charging characteristics at each temperature has been reported. The variation of constant current and constant voltage charging time with cycling, rate capability and impedance studies of both Sony 18650 cells and the electrode materials has been discussed in detail. This paper (Part II) deals with quantitative estimation of capacity loss with cycling and temperature. The study includes quantifying the capacity loss to three major factors namely rate capability loss, secondary active material ($LiCoO_2$/carbon) and primary active material (Li^+) losses. Intrinsic capacity measurements and XRD analysis of fresh and cycled electrode materials will also be discussed.

2. Experimental

Sony 18650 cells with 1.8 Ah rated capacity were used for all cycling studies. Table 1 shows the physical characteristics of the cell electrodes. The cells were charged with the same protocol as described in Part I of this paper. The temperatures chosen in this study were 45, 50 and 55 °C. Three cycle numbers 150, 300 and 800 were chosen to analyze the cycled cells. The instrumentation used and the cycling conditions are described in Part I of this paper. Rate capability studies were performed for the fresh cell as well as for the cycled cells. The cells were charged using the same CC–CV protocol as used for the cycling studies followed by discharging at different rates (*C*/9 to 1*C*).

The following studies were performed on the individual electrodes of the cell. The can of cycled Sony US18650S cells was carefully opened at fully discharged state in a glove box filled with ultra pure argon. Next, pellet or disc electrodes were made from the positive and negative electrodes of Sony 18650 cells and were used as working electrodes in the

* Corresponding author. Tel.: +1-803-777-7314; fax: +1-803-777-8265.
E-mail address: popov@engr.sc.edu (B.N. Popov).

0378-7753/02/$ – see front matter
PII: S0378-7753(02)00473-1

Table 1
Physical characteristics of Sony 18650 Li-ion battery electrodes

Characteristics	Positive $LiCoO_2$	Negative carbon
Mass of the electrode material (g)	13.4	5.7
Geometric area (both sides) (cm^2)	531	603
Loading on one side (mg/cm^2)	28.4	11.9
Thickness of the electrode (μm) (two side coating + current collector)	183	193
Dimensions of the electrode (cm × cm)	48.3 × 5.5	52.9 × 5.7

Table 2
Total capacity fade of Sony 18650 cells during several cycle numbers cycled at different temperatures

Q (capacity lost at different temperatures) (mAh)			
25 °C	45 °C	50 °C	55 °C
107 (150)	125 (150)	141 (150)	168 (150)
182 (300)	209 (300)	427 (300)	481 (300)
539 (800)	643 (800)	1074 (800)	1255 (490)

Numbers in brackets denote cycle number.

T-cell. Pure lithium metal was used as the counter and as reference electrode. Separator taken from the Sony 18650 cells was used as a separator in the T-cell. The diameter of the pellet electrodes was 1.20 cm. A 1 M $LiPF_6$ was used as the electrolyte in a 1:1 mixture of ethylene carbonate (EC), and di-methyl carbonate (DMC). X-Ray diffraction was done on both the $LiCoO_2$ and carbon electrodes. The patterns were collected at the end of discharge with a Tigaku 405S5 X-ray diffractometer using Cu Kα radiation.

3. Results and discussions

The rated capacity of the Li-ion cells used in this study is 1800 mAh. The cell was discharged using constant current of 1 A until the cell potential reaches the cut-off value of 2.0 V. A 5-min rest between charge and discharge and a 5-min rest between every cycle was applied to all batteries. Cycling studies were carried out at four different temperatures 25 °C (RT), 45, 50 and 55 °C. For cycling at RT, the cells were left in ambient conditions and for the other three temperatures, environmental chamber was used to control the temperature.

Fig. 1 represents a summary of the cycling performance of Sony 18650 cells that were discussed in detail in Part I of this paper. The figure shows the comparison of discharge curves

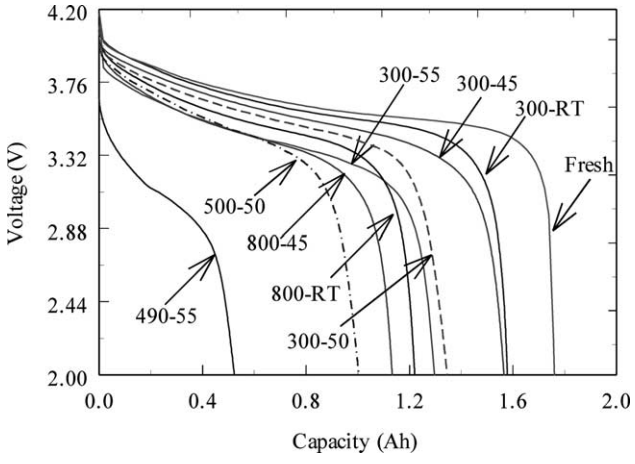

Fig. 1. Discharge curves of Sony 18650 cells cycled at different temperatures for various cycle numbers.

for the cells cycled at four temperatures. As shown in Fig. 1, the capacity fade is higher for the cell cycled at 55 °C when compared with the other two cells cycled at 50 and 45 °C. All cells showed a voltage drop which increases with cycling and temperature. After 490 cycles for the cell cycled at 55 °C the cell voltage immediately drops to around 3.7 V at the beginning of discharge. Similar drop in the cell voltage and higher capacity fade was observed for the cells cycled at 50 °C. This sudden drop in potential during the initial portion of the discharge curve indicates an increase in the high frequency impedance of the cell (dc resistance). After 800 cycles, the cells cycled at RT and 45 °C lost about 31 and 36% of their initial capacity, respectively. Cells at 50 °C were stopped cycling after 600 cycles since they lost more than 60% of initial capacity. Cells cycled at 55 °C showed a very high capacity loss of 70% after 500 cycles.

The cell cycled at RT showed a capacity fade of 31% after 800 cycles, which comes around to a capacity loss of 539 mAh. Similar calculations can be done for all temperatures for various cycles. Table 2 summarizes the total capacity lost at different cycle numbers when cycled at the four temperatures. The previous capacity fade studies [4,5] of commercial Li-ion cells, suggests several reasons namely increasing impedance of positive electrode, loss of active materials due to electrolyte oxidation, structural degradation of the positive electrode and so on for losing capacity with cycling under different cycling conditions.

Based on these conclusions and the data obtained from present work an attempt was made to quantify the total capacity loss due to several major factors. The three most significant parameters that we consider to cause the capacity loss are the rate capability, secondary active material ($LiCoO_2$/carbon) and primary active material (Li^+) losses. The total capacity fade is denoted as 'Q', which was obtained from the cycling data. The capacity fade balance can be represented as, $Q = Q_1 + Q_2 + Q_3$, where Q_1 represents the rate capability loss and other ohmic losses; Q_2 represents the capacity loss due to secondary active material and Q_3 refers to capacity loss due to Li-ion, which is the primary active material. Our objective was to provide appropriate estimations for each of these capacity fade parameters and to analyze the variation of these parameters with cycling as well as with temperature.

3.1. Estimation of Q_1 (rate capability losses)

From the analysis of charge and discharge curves it became clear that the increase in internal cell resistance causes large drop in cell voltage during discharge resulting in decrease in energy efficiency with cycling and temperature. The rate capability of the cell becomes poor due to higher resistance and hence capacity loss contributed by cell resistance increases with decreasing rate capability. In general rate capability can be defined as the maximum continuous or pulsed output current that a battery can provide. A Li-ion cell can be represented in electrical circuit terms as a voltage source in series with a resistance where the later parameter varies according to the electrochemical system, cell design as well as with the operating conditions.

The effect of ohmic drop and other cell resistances would be negligible when discharged at a sufficiently low rate (<*C*/5 rate) when compared with *C*/2 rate of discharge that was used to carry out cycling studies. Thus, to measure the rate capability losses, fresh and cycled cells at different temperatures were charged with the same CC–CV protocol as adopted for cycling studies, but discharged at different rates ranging from a very low rate of *C*/9 (0.2 A) to 1*C* rate (1.8 A). Fig. 5 of the first part of this paper presents the rate capability studies of Sony 18650 cells cycled at different temperatures. The difference in discharge capacity obtained for *C*/9 rate and *C*/2 rate would give us an estimate of rate capability loss. Based on the data presented in Fig. 5 of the Part I paper, we could able to estimate the capacity loss with cycling due to rate capability and Table 3 presents the rate capability losses (Q_1). From the data we could observe that for the first 150 cycles, the rate capability losses remains almost constant at all temperatures. With further cycling, the rate at which Q_1 increases is higher for the cells cycled at 50 and 55 °C when compared with other two temperatures.

Table 3
Rate capability losses of Sony 18650 cells cycled at different temperatures

Temperature (°C)	Cycle number	Rate capability losses Q_1 (mAh)
RT	150	28
	300	38
	800	71
45	150	27
	300	33
50	150	28
	300	62
	600	95
55	150	29
	300	81

3.2. Estimation of Q_2 (capacity loss due to degradation of active material)

Capacity fade due to active material degradation can be estimated from intrinsic capacity measurements. T-Cells were made for both positive ($LiCoO_2$) and negative (carbon) electrodes as working electrodes with Li metal being the counter and reference electrodes for each case. Low rate lithiation and de-lithiation experiments were done with these half-cells. The tests were done for the electrode materials taken from both fresh and cycled cells for all temperatures.

For the positive electrode, a constant current of about 8 mA/g was used for both lithiation and de-lithiation. The electrode taken from the fresh cell took about 18 h for complete charging and almost the same time for discharging. The potential limits were set to be 2.0 V for lithiation (discharging) and 4.2 V for de-lithiation (charging) for the positive electrode. Similarly, the potential limits for negative electrode were 2.0 V for de-lithiation (discharging) and 25 mV for complete lithiation (charging). Apart from the constant current lithiation, trickle charging was also done for the negative electrode when its potential reaches the lithiation cut-off value of 25 mV. This was done to make sure that the negative electrode was lithiated completely for specific capacity measurements as the Li-ion would find difficult to get intercalated even at very low currents due to the barriers caused by SEI layer or the passive film. Thus, for trickle charging the potential was held constant until the current drops to a value of approximately *C*/100 rate. For the negative electrode, a current of about 12 mA/g was used and this leads to charging the electrode from the fresh battery for 27 h. Such low rate was adopted for both positive and negative electrodes to eliminate any effects arising due to electrode resistance in order to get more accurate estimations for specific capacity. Since studies are done with Li foil as the counter electrode there are no capacity limitations due to the other electrode. Further, use of fresh electrolyte eliminates any losses arising due to the electrolyte evaporation in the battery. Hence, using this setup and studying $LiCoO_2$/carbon from cells at different cycles, it is possible to analyze losses from the secondary active material $LiCoO_2$/carbon electrode alone.

Fig. 2 presents the lithiation and de-lithiation curves for $LiCoO_2$ electrode taken from a fresh and cycled Sony 18650 cells. The lithiation curve for the fresh $LiCoO_2$ electrode appears almost flat till the end of discharge when compared to that of cycled electrode where the profile is very steep with continuous drop in electrode potential till the end of discharge. Fig. 3 shows the charge (de-lithiation) and discharge (lithiation) curves of fresh and cycled carbon electrode. There is no significant change in the discharge curves of fresh and cycled electrode materials. But the intrinsic capacity of the cycled electrode was found to be lower than that of fresh electrode.

Table 4 shows the specific capacity values obtained from T-cell measurements for both positive and negative electrodes taken from the cells cycled at all temperatures. It is seen that the $LiCoO_2$ from the fresh battery has a capacity of 148 mAh/g. The capacity here is normalized to the total weight of the disc electrode that includes binder and other additives minus the weight of the current collector. After 300 cycles at 55 °C, the active material capacity goes down to

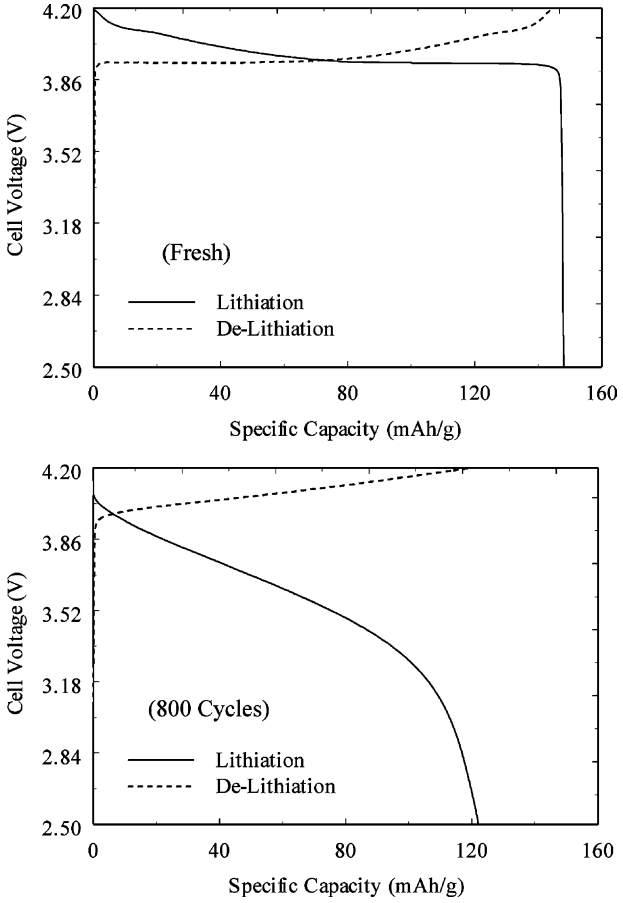

Fig. 2. Charge and discharge curves of $LiCoO_2$ electrode taken from fresh and cycled Sony 18650 cells.

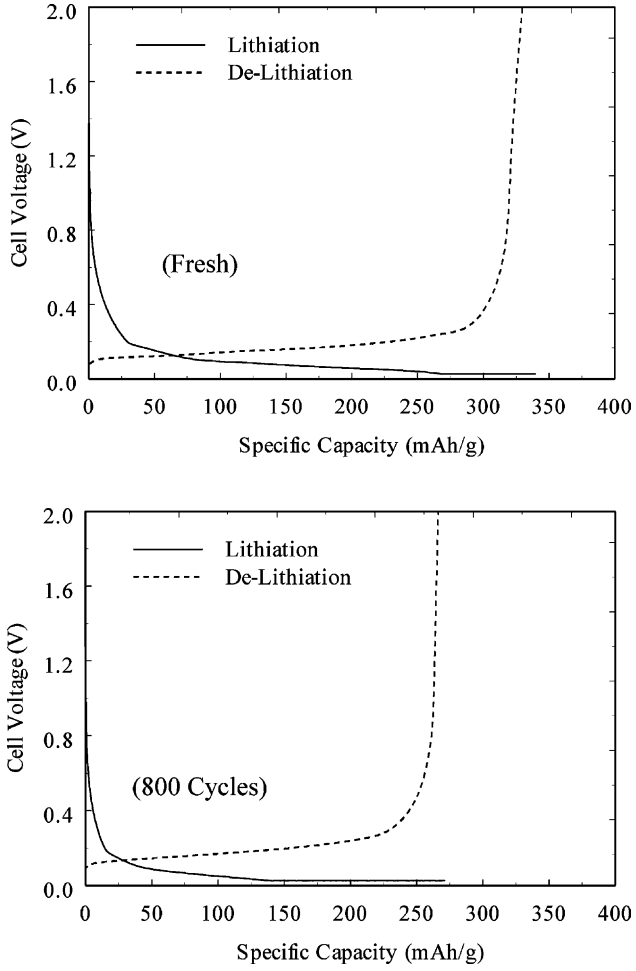

Fig. 3. Charge and discharge curves of carbon electrode taken from fresh and cycled Sony 18650 cells.

131 mAh/g. These results indicate that part of the $LiCoO_2$ is converted to an inactive form with cycling. As shown in Table 4 increasing temperature contributes to more loss of $LiCoO_2$. Similar results are also seen for carbon electrode. However, in this case a much higher loss is seen after 300 cycles at 55 °C. For electrodes taken from the cells cycled at RT and 45 °C, the percentage decrease in the specific capacity of positive electrode was higher than that of the negative electrode up to 300 cycles. For the other two temperatures, the decrease in the negative electrode capacity was higher than the positive electrode after 150 cycles. These half-cell results are consistent with the full-cell cycling results where for the first 200 cycles, the decrease in the capacity with cycling is similar for all cells. Beyond 200 cycles, there is an increased rate of capacity fade for the cells cycled at 50 and 55 °C. Based on the amount of active material loading and the intrinsic capacity values, the secondary active material losses were calculated with carbon being the limiting electrode for capacity loss measurements. The secondary active material loss is also tabulated in Table 4.

Table 4
Variation of specific capacity of $LiCoO_2$ and carbon electrode and secondary active material loss with cycling and temperature

Temperature (°C)	Cycle number	Specific capacity (mAh/g)		Secondary active material loss Q_2 (mAh)
		$LiCoO_2$	Carbon	
	Fresh	148.13	339.90	
RT	150	145.61	334.03	33
	300	141.07	325.04	85
	800	122.14	271.10	392
45	150	143.74	332.84	40
	300	139.26	325.71	81
50	150	143.28	331.20	65
	300	133.56	293.91	262
	600	94.05	202.53	783
55	150	142.84	328.90	63
	300	131.13	286.92	302

3.3. XRD analysis of electrode materials

To analyze whether there is any change in electrode structure with cycling X-ray diffraction studies were done for fresh as well as cycled electrode materials. Fig. 4 presents the XRD patterns of the completely lithiated positive electrode from

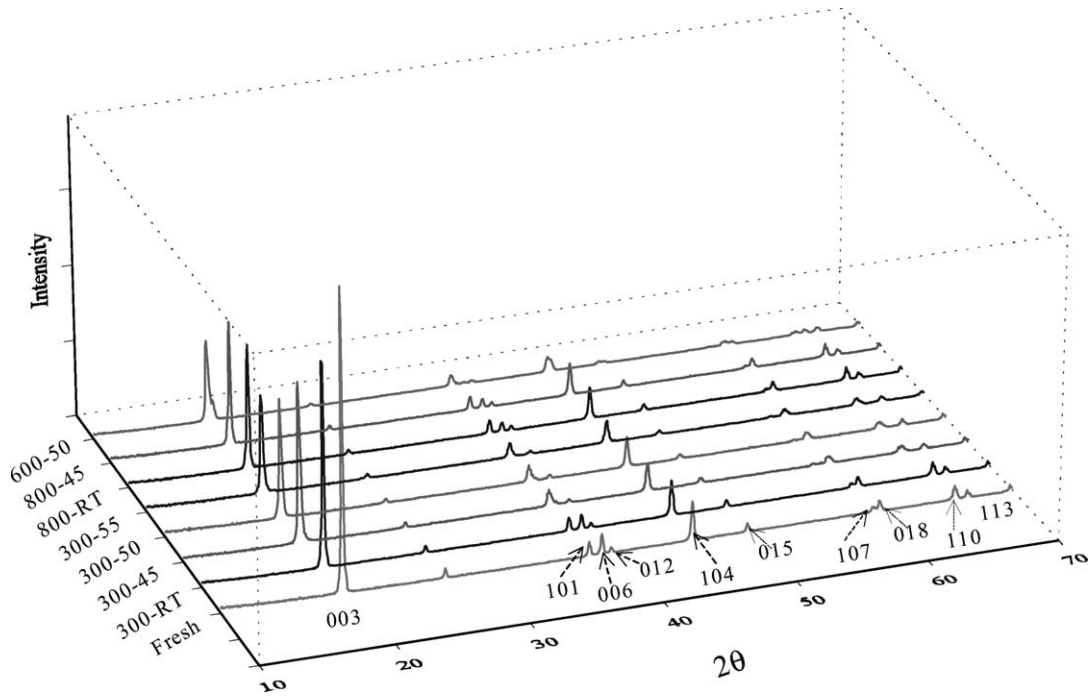

Fig. 4. XRD patterns of $LiCoO_2$ electrodes taken from Sony 18650 cells cycled at different temperatures.

different cells. All the XRD patterns show a perfect crystalline structure with all peaks indexable in the hexagonal lattice [6]. From the XRD patterns we could observe that with cycling and temperature, the appeared characteristic peaks of the $LiCoO_2$ remain the same, which indicates that no new phase is formed. But the peak intensities of (0 0 3), (0 0 6) and (1 0 4) planes are different among the XRD pattern that indicates a change in the structure of the $LiCoO_2$ phase [7] with cycling at different temperature. In the $LiCoO_2$ phase, alternate layers of Li and Co cations occupy the octahedral sites of a compact close packing of oxide anions. The (0 0 3) peak intensity decrease occurs when a cobalt atom occupies some of the octahedral sites of the lithium layer [8]. Hence a decrease in the relative intensity of the (0 0 3) peak during cycling indicates that the cation in the well-layered $LiCoO_2$ becomes disordered and a portion of the Li-ions in the cathode becomes inactive. Moreover, from the XRD patterns it was found that peaks start to shift to higher 2θ values with cycling as well as with temperature. This results in a variation in the lattice parameters '*a*' and '*c*' and hence a decrease in the *c*/*a* ratio with cycling and temperature. The decrease in the *c*/*a* ratio indicates a decrease in the lithium stoichiometry with cycling.

Yoon et al. [9], performed XAS analysis in the $LiCoO_2$ film electrode and their results show that for a cycled $LiCoO_2$ electrode, capacity fading could be related to the decrease in the Co–O bond covalency by the local structural distortion of Co site remaining in the cycled $LiCoO_2$. They suggest that the Li-ion deintercalation leads to the local distortion of CoO_6 octahedral symmetry and the charge compensation for the electron exchange in the Li-ion de-intercalation–intercalation process is achieved mainly at the oxygen site as well as the Co atomic site. Nakai et al. [10] reported from their in situ Co K-edge XANES spectra of $Li_{1-x}CoO_2$ that a positive shift in energy for the absorption spectrum reflects the progressive oxidation of the Co^{3+} ion to the Co^{4+} ion in $Li_{1-x}CoO_2$ with the deintercalation of Li and also accounts for the shortening of the Co–O distance. These observations support the conclusions we made based on the XRD patterns of fresh and cycled positive electrode materials.

XRD studies were also done for fresh and cycled negative electrode materials and Fig. 5 presents the XRD patterns of the cycled negative electrode at the four temperatures compared with that of the fresh one. From the patterns it was quite clear that the negative electrode material is a graphitized carbon because of the strong (0 0 2) peak. While comparing the XRD patterns with that of the fresh electrode, no change was observed with the intensities or positions of the characteristic peaks of the carbon electrodes with cycling at different temperature. With the XRD patterns of carbon electrode no significant conclusion could be drawn whether there is any degradation or new phase formation in the electrode material.

3.4. Estimation of Q_3 (capacity fade due to primary active material loss)

From the specific capacity measurements carried out on electrodes taken from the fresh cell, it was found that the cell was limited by negative electrode. The decrease in the specific capacity of carbon taken from the cell cycled 800 times at RT was found to be 20.24% and this is equivalent to a capacity loss of about 392 mAh based on the total amount of negative electrode active material. From the cell capacity fade studies, after 800 cycles, the actual capacity was 539 mAh, while the rate capability losses were estimated to

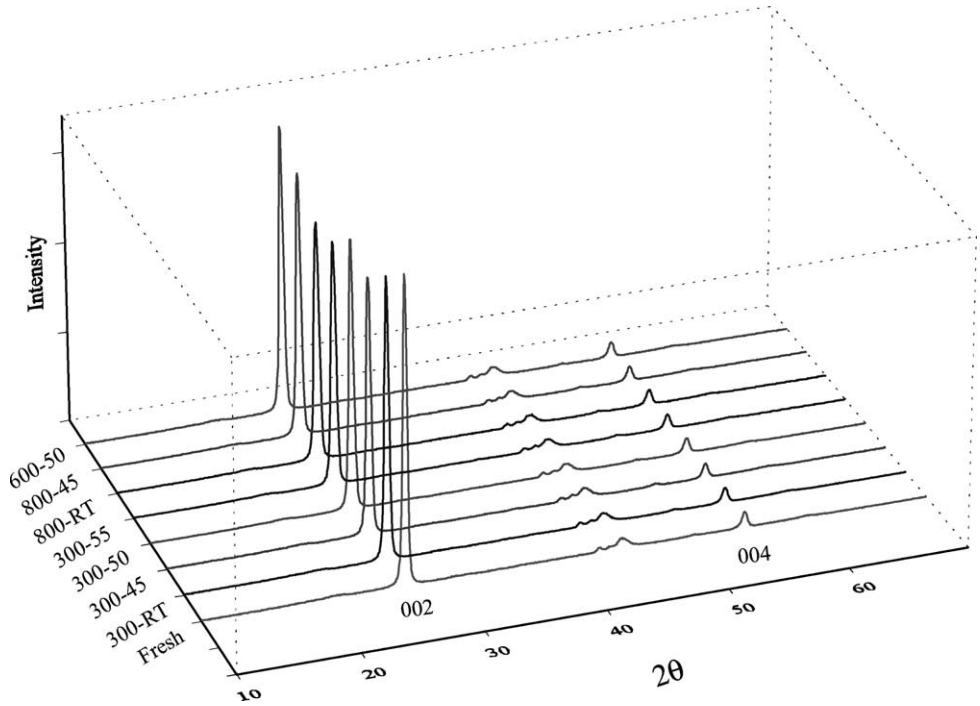

Fig. 5. XRD patterns of carbon electrodes taken from Sony 18650 cells cycled at different temperatures.

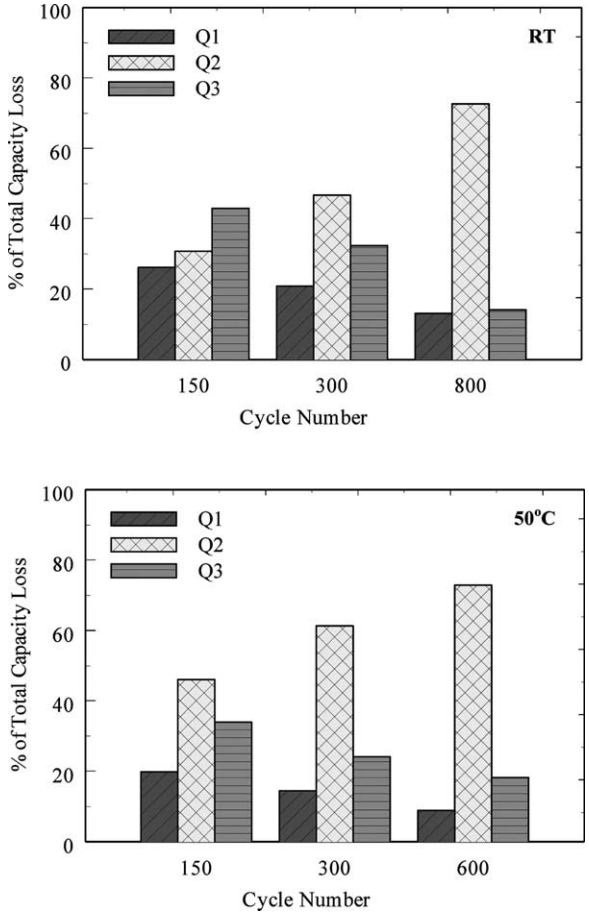

Fig. 6. Percentage variation of the capacity fade factors (Q_1, Q_2, Q_3) at various cycles for the cells cycled at RT and 50 °C.

be 71 mAh. Thus, the remaining 76 mAh of the lost capacity as obtained from charge balance ($Q - Q_1 - Q_2$) can be attributed to primary active material (Li^+) loss. The same calculation holds for the cells cycled at other temperatures. Fig. 6 summarizes the distribution of capacity losses between the secondary active material ($LiCoO_2$/carbon) losses, primary active material (Li^+) loss and capacity loss due to rate capability for cells cycled at RT and 50 °C. For cells cycled at RT, after 150 cycles all three capacity fade factors contribute almost equally to the total capacity loss. However, with further cycling, secondary active material loss was dominating among the three and continues to remain higher after 800 cycles. For cells cycled at 50 °C, the primary active material loss was comparable to secondary active material loss (Q_2) for 150 cycles, but with further cycling, Q_2 remains highest. Note that lithium loss (Q_3) is lower for cycling at RT when compared with cycling at elevated temperatures.

4. Conclusion

A complete capacity fade analysis was carried out for Sony 18650 cells cycled at elevated temperatures. The major causes for capacity loss were categorized as rate capability loss, primary and secondary active material losses. Rate capability measurements were used to estimate the capacity loss due to a decrease of the Li^+ transference number. Charge–discharge studies on individual pellet electrodes show a reduced tendency for lithiation for both $LiCoO_2$ and carbon with continuous cycling. Intrinsic capacity measurements for both positive and negative electrode were used

to estimate the capacity loss due to secondary active material and a charge balance gives the capacity lost due to primary active material (Li^+). XRD studies of the $LiCoO_2$ electrode showed a decrease in the lithium stoichiometry with cycling while no significant structural changes have been identified with XRD patterns of carbon electrode. The higher capacity fade for the cells cycled at higher temperatures was due to a repeated film formation over the surface of anode which results in increase rate of lithium loss and also a large increase in negative electrode resistance with cycling. Capacity fade balance indicated that secondary active material loss dominates the other losses (Li^+-ion loss and rate capability losses) irrespective of cycling temperature.

Acknowledgements

Financial support provided by (NRO) National Reconnaissance office, under contract number NRO-00-C-0134 is acknowledged gratefully.

References

[1] P. Arora, R.E. White, M. Doyle, J. Electrochem. Soc. 145 (1998) 3647.
[2] J.R. Dahn, E.W. Fuller, M. Obravae, U. Von Sacken, S. S. Ionics 69 (1994) 265.
[3] E. Peled, Lithium stability and film formation in organic and inorganic electrolyte for lithium battery systems, in: J.P. Gabano (Ed.), Lithium Batteries, Academic Press, New York, 1983.
[4] D. Zhang, B.S. Haran, A. Durairajan, R.E. White, Y. Podrazhansky, B.N. Popov, J. Power Sources 91 (2000) 122.
[5] P. Ramadass, A. Durairajan, B.S. Haran, R.E. White, B.N. Popov, J. Electrochem. Soc. 149 (1) (2002) A54.
[6] G.T.-K. Fey, V. Subramanian, J.-G. Chen, Electrochem. Commun. 3 (2001) 234.
[7] J. Li, E. Murphy, J. Winnick, P.A. Kohl, J. Power Sources 102 (2001) 302.
[8] E.-D. Jeong, M.-S. Won, Y.-B. Shim, J. Power Sources 70 (1998) 70.
[9] W. Yoon, K. Kim, M. Kim, M. Lee, H. Shin, J. Lee, C. Yo, J. Phys. Chem. B 106 (2002) 2526.
[10] I. Nakai, K. Takahashi, Y. Shiraishi, T. Nakagome, F. Nishikawa, J. Solid State Chem. 140 (1998) 145.